Electrochimica Acta, Vol. 37, No. 12, pp. 2209–2214, 1992
Printed in Great Britain.

0013–4686/92 $5.00 + 0.00
© 1992. Pergamon Press Ltd.

A COMPARATIVE STUDY OF ELECTRODEPOSITED AND VAPOUR DEPOSITED GOLD FILMS: FRACTAL SURFACE CHARACTERIZATION THROUGH SCANNING TUNNELLING MICROSCOPY

P. Herrasti,* P. Ocón,* R. C. Salvarezza,* J. M. Vara,* L. Vázquez† and A. J. Arvia‡

*Departamento de Química-Física Aplicada, C-II, Universidad Autónoma de Madrid, 28049 Madrid, Spain

†Instituto de Ciencias de Materiales, Sede B, CSIC Departamento de Física Aplicada, C-XII, Universidad Autónoma de Madrid, Spain

‡INIFTA, Universidad Nacional de La Plata, Sucursal 4, Casilla de Correo 16, (1900) La Plata, Argentina

(*Received* 30 *January* 1992)

Abstract—The surfaces of Au deposits grown under non-equilibrium conditions from either the electroreduction of Au oxide or from the vapour have been analysed as fractals by measuring the perimeter (P) and the area (A) of intergranular voids. The values of P and A were determined from scanning tunnelling microscopy (STM) topographic imaging of the deposit surfaces. A fractal behaviour $P \propto A^{D/2}$ was found with $D = 1.5 \pm 0.1$ and $D = 1.7 \pm 0.1$ for the electrodeposited and vapour deposited Au films, respectively. These figures remain constant for film thicknesses between 100 and 1000 nm. The value of D_s, the fractal dimension of the surfaces, is 2.5 ± 0.1 for the Au electrodeposits, and 2.7 ± 0.1 for the Au vapour deposited films. The former value is consistent with either a diffusion or an electric field controlled growth model, whereas the latter is in agreement with a ballistic growth model.

Key words: fractal surfaces, scanning tunneling microscopy, electrocrystallization, metal vapour deposition, gold electrodes.

INTRODUCTION

Metal deposition belongs to a wide class of aggregation phenomena[1]. The growth of metal deposits far from equilibrium leads to either dendritic, columnar, diffusion-limited or dense radial patterns, according to the operating conditions[2]. In many cases these patterns are better described as fractal rather than Euclidean objects[1]. However, the demonstration of fractality for real systems is difficult because the fractal behaviour can be observed only within certain scale lengths by using appropriate experimental methods[3]. In addition, the parametric relationships used to obtain the fractal dimension of an object are mostly applicable to self-similar fractals, despite the fact that a large number of real systems involve anisotropic properties, and accordingly should be described as self-affine fractals[1, 4]. Therefore, often the self-similar character or the self-affine character of the object is difficult to demonstrate unambiguously.

Recently, a STM method which can be applied to both self-similar and self-affine fractals has been developed to obtain the fractal dimension of conducting surfaces at the nanometre scale[5]. The method is based on the fact that the intersection of a plane with either a self-similar or a self-affine fractal surface generates self-similar lakes or islands. Correspondingly, the fractal dimension can be obtained from the perimeter (P) *vs* area (A) relationship of the generated lakes[1]. Using this method D_s, the fractal dimension of surfaces of Au electrodeposits of thickness close to 1000 nm was evaluated ($D_s = 2.5$), and the influence of surface rearrangements on D_s was determined[5].

This paper describes the fractal characterization of Au deposits prepared by different methods at similar high growth rates, substrate temperature and film thickness. For this purpose, Au electrodeposits grown from the electroreduction of gold oxides and Au films prepared through vapour deposition on glass have been employed. A good correlation between the experimental D_s values and those obtained from computer simulation based on different growth models was found for each type of Au deposit.

EXPERIMENTAL

Electrochemically and vapour deposited Au films were grown under conditions far from equilibrium at 298 K up to average film thicknesses, h, ranging from 30 to 1200 nm. The electrochemically deposited Au films (hereafter denoted AuEDE) were prepared at a growth rate $v = 100\ \mathrm{nm\ s^{-1}}$ by electroreducing relatively thick hydrous Au oxide layers accumulated on a Au wire electrode in 0.5 M H_2SO_4. Further details about the preparation procedure of AuEDE are given in Ref[6]. The Au electrodeposits look like "black deposits" to the open eye, and they exhibit a structure made of pores and channels as seen through SEM micrographs.

Vapour deposited Au films (hereafter denoted AuVDE) were grown at $v = 30\ \mathrm{nm\ s^{-1}}$ on smooth

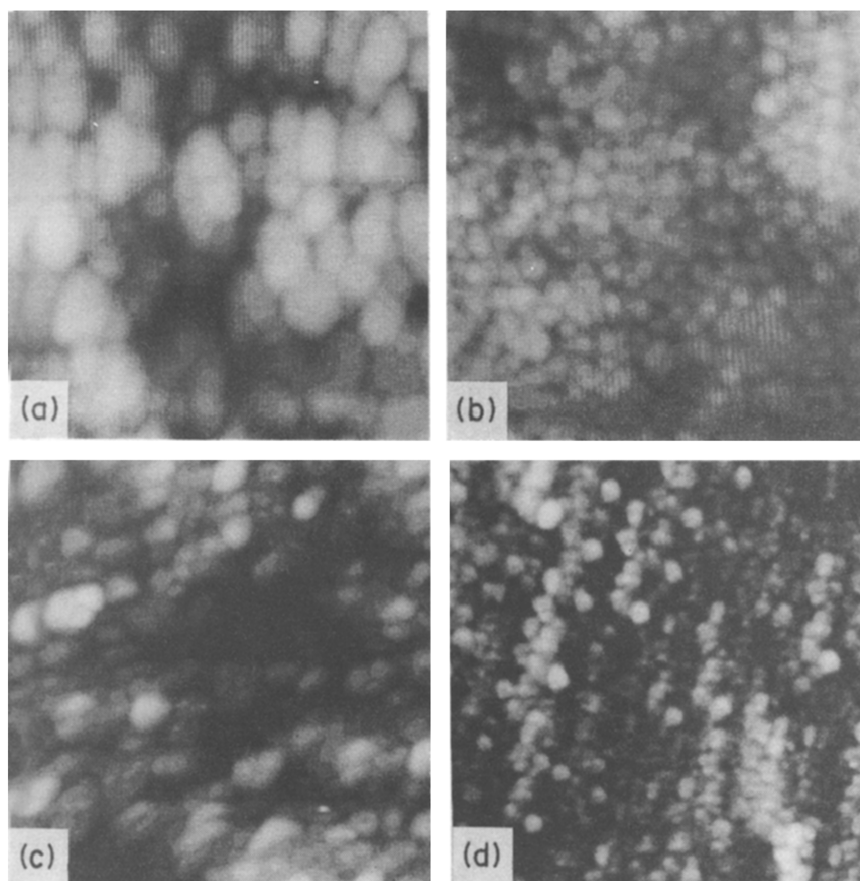

Fig. 1. STM grey scale images of Au deposits. Au electrodeposits: (a) 400 × 400 nm^2; (b) 1000 × 1000 nm^2. Vapour deposited Au: (c) 500 × 500 nm^2; (d) 1600 × 1600 nm^2.

glass substrates (1 × 3 cm rectangular pieces), using an evaporator chamber with a nearly 90° incident particle direction with respect to the substrate plane. The AuVDEs appear rather smooth even through SEM imaging at × 10,000.

The surface area (S) of the Au deposits was determined through the O adatom electrodesorption voltammetric charge in 0.5 M H_2SO_4 at 0.1 V s^{-1} between 0.05 and 1.65 V. The charge density of the O atom monolayer on polycrystalline Au was taken equal to 0.42 mC cm^{-2}[7].

For using the AuVDE as working electrodes the following mounting was employed. One half of the rectangular piece was immersed in the electrolyte solution, becoming the active working electrode area, whereas electrical contact was made at the upper part of the piece outside the solution, by clamping to a Cu wire which was protected with Teflon. This experimental arrangement provided a very reproducible and stable voltammetric response in O_2-free 0.5 M H_2SO_4 under the above-mentioned conditions. The corresponding voltammograms closely resemble those resulting on Au(111) single crystal electrodes. The AuVDE(111) preferred crystallographic orientation was confirmed through X-ray diffractometry data[8].

Typical values of S for AuEDE and AuVDE deposits of $h = 1000$ nm are 80 and 4 cm^2 per square centimetre apparent substrate area, respectively. The roughness factor (R) of the Au deposits was defined by:

$$R = S/S_s, \quad (1)$$

where S_s stands for the geometric area of the substrate.

STM measurements were made using a piezotube-type microscope operating in air. Tips were obtained by cutting 0.2 mm diameter Pt wires. All measure-

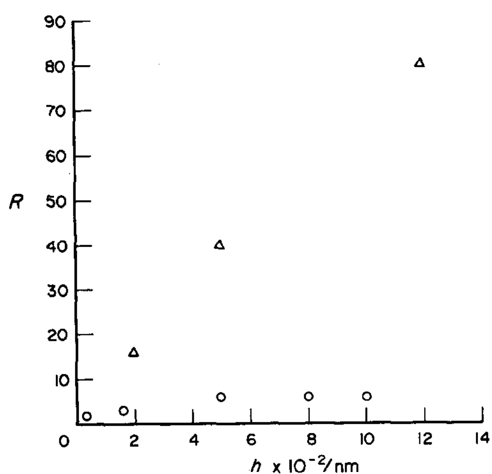

Fig. 2. R *vs* h plot for (△) Au electrodeposits and (○) vapour deposited Au films.

ments were made at the constant current mode with a bias voltage between 0.05 and 0.1 V, and a tunnelling current between 1 and 2 nA. Data were acquired by a fully automated work station and stored as digitized images. In all cases the STM measurements were made immediately after the Au deposit preparation to avoid surface rearrangements caused by surface atom diffusion[5, 9].

RESULTS AND DISCUSSION

The STM grey scale images of AuEDE and AuVDE at two different magnifications are shown in Fig. 1a–d respectively. The STM images of both AuEDE and AuVDE appear similar at the nanometre level, exhibiting small rounded grains and branched voids. The average grain size for both deposits is close to 40 nm, however the characteristics of the surfaces are rather different as seen from the dependence of the corresponding roughness factor on the film thickness (Fig. 2). Thus, for the AuEDEs a nearly linear R *vs* h plot is obtained indicating an open structure with voids and channels penetrating deeply in the deposit structure. Otherwise, for the AuVDEs R increases slightly with h and finally reaches a practically constant value (Fig. 2). This means that the AuVDE structure is more compact, *ie*

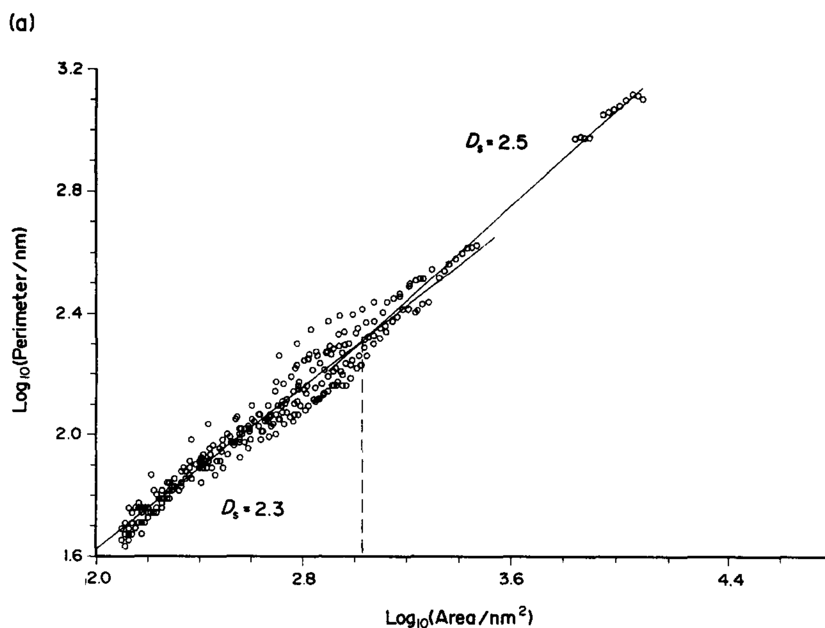

Fig. 3(a)

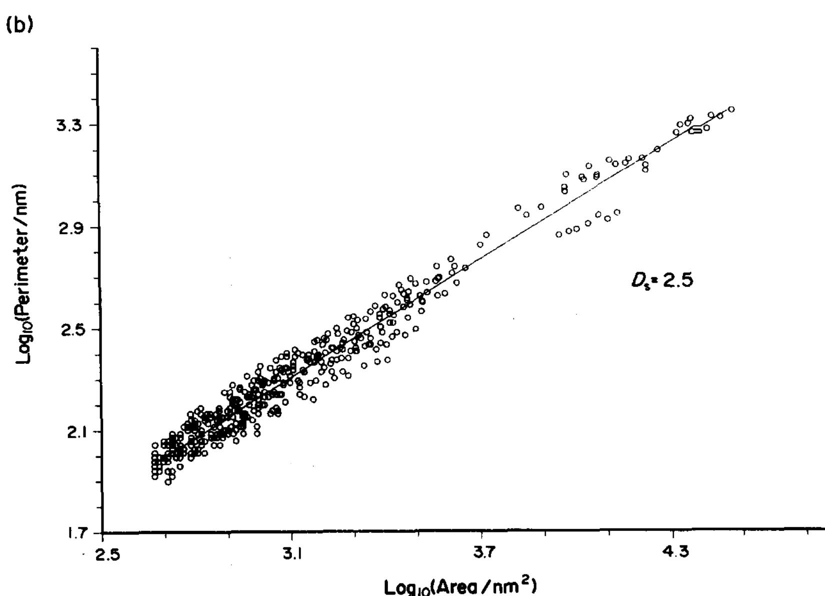

Fig. 3(b) (*continued overleaf*)

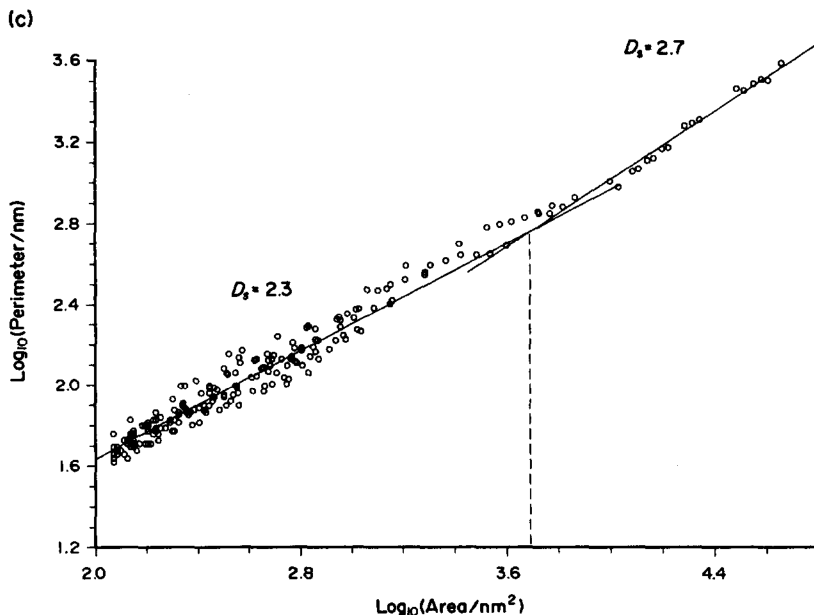

Fig. 3(c)

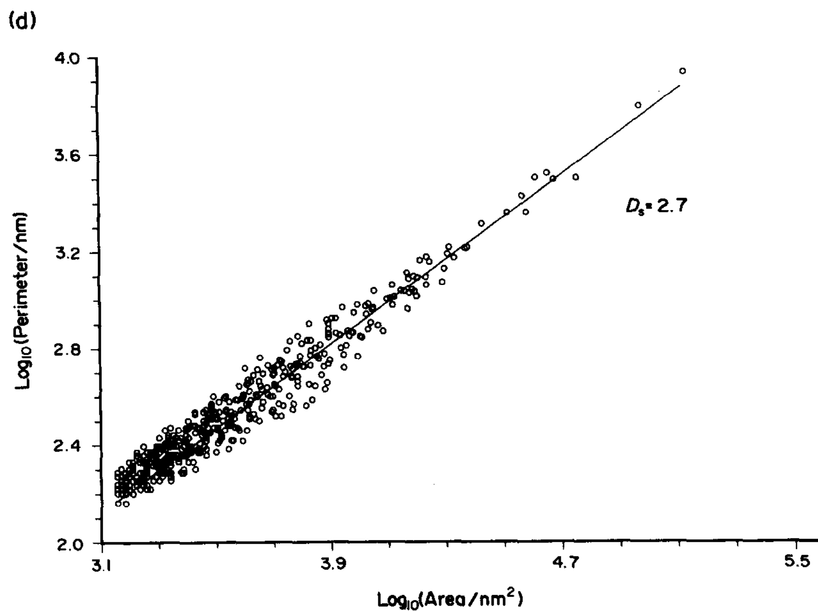

Fig. 3(d)

Fig. 3. (a) log P *vs* log A plot for the lakes generated by filling with "water" the images shown in Fig. 1a; (b) log P *vs* log A plot for the lakes generated by filling with "water" the image shown in Fig. 1b; (c) log P *vs* log A plot for the lakes generated by filling with "water" the image shown in Fig. 1c; (d) log P *vs* log A plot for the lakes generated by filling with "water" the image shown in Fig. 1d.

voids and channels penetrate only a few nanometres in the deposit.

The fractal surface dimension of Au deposits was determined through the area (A)–perimeter (P) analysis of the corresponding digitized STM images. In a way similar to that described for the earth coastlines[1], the surface topography (Fig. 1a–d) was filled with "water" up to a preset level to simulate lakes; then the values of P and A of every lake were obtained. The value of P was defined as the number of "water" pixels on the digitized grid having "no water" neighbours, whereas the value of A was defined as the number of "water" pixels. A pixel is defined as the smallest element of an image that can be individually processed in a video display system. The yardstick value (δ) of the digitized grid is given by the ratio between the total scanned area and the number of pixels in the image (256×256). As the

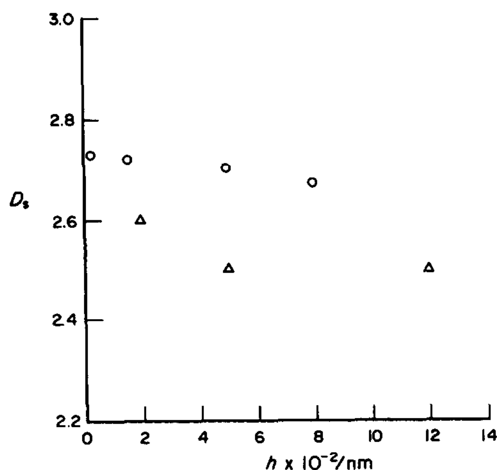

Fig. 4. D_s *vs* h plots for (△) Au electrodeposits and (○) vapour deposited Au layers.

measurements of P and A for a lake in the digitized image require δ to be sufficiently small to account for the smallest features [10], only lakes with A greater than $30\delta^2$ were considered.

As the intersection of a plane with either a self-similar or a self-affine surface generates self-similar lakes, one can relate P and A through the following equation[1, 4]:

$$P(\delta) = \alpha D A^{D/2}, \quad (2)$$

where α is a constant and D is the fractal dimension of the void perimeter. Thus, D can be calculated from the log P *vs* log A plot. From the STM images at lower magnification (Fig. 1b–d), only straight lines involving $D = 1.5 \pm 0.1$ for AuEDE, and $D = 1.7 \pm 0.1$ for AuVDE (Fig. 3b–d) can be obtained. However, from the STM images taken at large magnification (Fig. 1a–c), the log P *vs* log A plots for both AuEDE and AuVDE yield two straight lines whose intersection defines an inner cut-off, λ (Fig. 3a–c). $A < \lambda$ results in $D = 1.3 \pm 0.1$ for both types of Au deposits, whereas for $A > \lambda$ one obtains $D = 1.5 \pm 0.1$ and $D = 1.7 \pm 0.1$ or AuEDE and AuVDE, respectively (Fig. 3a–c). It should be noted that the high slopes in Fig. 3a–c are justified by data resulting in plots shown in Fig. 3b and d starting from log $A = \lambda$ upwards. These results indicate that two kinds of lakes have been generated at Au deposit surfaces. The smallest lakes are rounded in shape, with a lower fractal dimension ($D = 1.3 \pm 0.1$), in contrast to the biggest ones which are highly ramified and have larger fractal dimensions ($D = 1.5 \pm 0.1$ and $D = 1.7 \pm 0.1$), depending on the type of Au deposit. As reported earlier[5], results obtained by using different probing tips yield the same values of D within ± 0.1. The physical meaning of λ which is related to the average particle size, is discussed in detail elsewhere[8].

The fractal dimension of the deposit surface (D_s) is related to D through the relationship[1]:

$$D = D_s - 1. \quad (3)$$

Accordingly, from equation (2) and $A > \lambda$, one obtains $D_s = 2.5 \pm 0.1$ for AuEDE, and $D_s = 2.7 \pm 0.1$ for AuVDE. On the other hand, for $A < \lambda$ both types of deposits exhibit $D_s = 2.3 \pm 0.1$.

The D_s *vs* h plots for AuVDE and AuEDE are shown in Fig. 4. The values of D_s remain practically constant in the $100\,\text{nm} < h < 1200\,\text{cm}$ range. These results reveal that no change in the fractal characteristics of the Au deposits occurs in going from the earlier to the advanced stages of the Au overlayer growth. Therefore, a single value of D_s describes the geometry of the growing metal surface.

Let us now attempt to correlate the values of D_s with the probable growth mechanism for both types of Au deposit. The value $D_s = 2.7 \pm 0.1$ obtained for AuVDE is very close to $D_s = 2.67$ as predicted from large-scale 3-D computer simulations of ballistic models[11]. Accordingly, particles impinging the growing interface at random aggregate exactly at the impinging sites without reconstruction. This process leads to a compact structure with a self-affine fractal surface characterized by the value $D_s = 2.67$[12]. This description is consistent with both STM images and conclusions drawn from the R *vs* h plots. Therefore, in principle, the ballistic model appears to be adequate for describing the growth process of AuVDE.

On the other hand, the value of $D_s = 2.5 \pm 0.1$ found for AuEDE coincides with the predictions of 3-D computer simulations of DLA, the diffusion-limited aggregation model[3]. In this case a rough surface with deep voids and channels interconnecting the entire deposit structure is expected. This picture is consistent with the STM images and the R *vs* h plot obtained for this type of electrodeposit. It should be noted that values of $D = 2.5 \pm 0.1$ were also obtained for Cu and Ag dendritic electrodeposited surfaces[13, 14].

The SEM micrographs of AuEDE cross-sections indicate that a self-affine rather than a self-similar fractal structure is perhaps a better description for the AuEDE surfaces[15]. It should be noted that diffusion limited deposition models can also lead to the development of anisotropic patterns due to cluster competition for growth[12]. Furthermore, the DLA model itself captures the essential fractal features of a wide range of physical phenomena such as electrochemical deposition, particle aggregation, electric breakdown and viscous fingering[16] for which the interface motion is dominated by a quantity satisfying the Laplace equation.

CONCLUSIONS

The area–perimeter STM method which has been developed to evaluate the fractal dimension of rough surfaces was applied to characterize the fractal geometry of the surfaces of Au electrodeposits and Au vapour deposited films both grown at comparable high deposition rates and substrate temperature. For $A > \lambda$, $D_s = 2.5 \pm 0.1$ and $D_s = 2.7 \pm 0.1$ for Au electrodeposits and vapour deposited Au films, respectively. As the D_s values remain unchanged with deposited film thickness, the same mechanism of growth seems to operate in the $100\,\text{nm} < h < 1000\,\text{nm}$ thickness range. These figures also reflect different growth mechanisms of the Au layer at the

Au oxide/Au metal electrochemical interface and at the Au vapour/Au metal interface. In the former case, the Au layer growth can be described throughout diffusion limited deposition models, whereas for the latter ballistic deposition models appear to be the most appropriate ones.

Acknowledgements—Financial support for this research work obtained from MAT89-0204 (CICYT, Spain) is acknowledged. R.C.S. thanks CICYT (Spain) and CONICET (Argentina) for the fellowships granted.

REFERENCES

1. B. B. Mandelbrot, *The Fractal Geometry of Nature*, Freeman, San Francisco (1977).
2. D. G. Grier, D. A. Kessler and L. M. Sanders, *Phys. Rev. Lett.* **59**, 2315 (1987).
3. P. Meakin, in *The Fractal Approach to the Heterogeneous Chemistry* (Edited by D. Avnir), Wiley, New York (1989).
4. J. Feder, *Fractals*, Plenum Press, New York (1988).
5. J. Gómez-Rodríguez, A. M. Baró, L. Vázquez, R. C. Salvarezza, J. M. Vara and A. J. Arvia, *J. phys. Chem.* **96**, 347 (1992).
6. A. C. Chialvo, W. E. Triaca and A. J. Arvia, *J. electroanal. Chem.* **71**, 303 (1984).
7. S. Trasatti and O. A. Petrii, *Pure appl. Chem.* **67**, 711 (1991).
8. P. Herrasti, P. Ocón, L. Vázquez, R. C. Salvarezza, J. M. Vara and A. J. Arvia, *Phys. Rev. A*, in press.
9. C. Alonso, R. C. Salvarezza, J. M. Vara, A. J. Arvia, L. Vázquez, A. Bartolomé and A. M. Baró, *J. electrochem. Soc.* **137**, 2161 (1990).
10. B. H. Kaye, in *The Fractal Approach to the Heterogeneous Chemistry* (Edited by D. Avnir), Wiley, New York (1989).
11. P. Meakin, *J. Phys. A.* **20**, 1113 (1987).
12. T. Vicsek, *Fractal Growth Phenomena*, World Scientific, London (1989).
13. R. M. Brady and R. C. Ball, *Nature* **309**, 225 (1984).
14. A. Hernández-Creus, P. Carro, R. C. Salvarezza and A. J. Arvia, *J. electrochem. Soc.*, in press.
15. M. Gómez, L. Vázquez, R. C. Salvarezza, J. M. Vara and A. J. Arvia, *J. electroanal. Chem.* **317**, 125 (1991).
16. B. B. Mandelbrot and C. J. Evertsz, *Nature* **348**, 143 (1990).